






ARTICLE OPEN



Mesenchymal stromal cells equipped by IFN α empower T cells with potent anti-tumor immunity

Tao Zhang¹, Yu Wang¹ , Qing Li¹, Liangyu Lin¹ , Chunliang Xu¹ , Yueqing Xue¹, Mingyuan Hu¹, Yufang Shi^{1,2}  and Ying Wang¹ 

© The Author(s) 2022

Cancer treatments have been revolutionized by the emergence of immune checkpoint blockade therapies. However, only a minority of patients with various tumor types have benefited from such treatments. New strategies focusing on the immune contexture of the tumor tissue microenvironment hold great promises. Here, we created IFN α -overexpressing mesenchymal stromal cells (IFN α -MSCs). Upon direct injection into tumors, we found that these cells are powerful in eliminating several types of tumors. Interestingly, the intra-tumoral injection of IFN α -MSCs could also induce specific anti-tumor effects on distant tumors. These IFN α -MSCs promoted tumor cells to produce CXCL10, which in turn potentiates the infiltration of CD8⁺ T cells in the tumor site. Furthermore, IFN α -MSCs enhanced the expression of granzyme B (GZMB) in CD8⁺ T cells and invigorated their cytotoxicity in a Stat3-dependent manner. Genetic ablation of Stat3 in CD8⁺ T cells impaired the effect of IFN α -MSCs on GZMB expression. Importantly, the combination of IFN α -MSCs and PD-L1 blockade induced an even stronger anti-tumor immunity. Therefore, IFN α -MSCs represent a novel tumor immunotherapy strategy, especially when combined with PD-L1 blockade.

Oncogene (2022) 41:1866–1881; <https://doi.org/10.1038/s41388-022-02201-4>

INTRODUCTION

The tumor microenvironment contains multiple types of immune cells, such as T cells, B cells, macrophages, and neutrophils, as well as tumor stromal cells, including fibroblasts, endothelial cells, and mesenchymal stromal cells [1]. These nonmalignant cells not only facilitate tumor growth and progression, but also strongly affect the efficiency of various cancer treatments [2–4]. Strategies targeting immune checkpoints, such as PD-L1 and CTLA-4, have been shown to restore the function of exhausted CD8⁺ T cells and have demonstrated impressive efficacy in some patients suffering from various cancer types. However, the majority of cancer patients do not acquire durable benefit [5]. Therefore, novel tumor microenvironment modulating strategies are still to be formulated to effectively eradicate tumors.

It has been demonstrated that preexisting infiltrated T cells in the tumor microenvironment are a good prognosis marker for cancer treatment [6–8]. According to the immune contexture, tumors can be classified into “hot” (inflamed) and “cold” (non-inflamed) tumors [9, 10]. The immune features of “hot” tumors are a good indicator for the utility of immune checkpoint blockades. However, the abundance of stromal cells within tumors could significantly affect the infiltration of T cells in the tumors [11]. When a tumor was found to possess less infiltrated immune cells, more resident immunosuppressive cells, or abundant immune cells in surrounding tissues, a poor prognosis of the treatment of immune checkpoint blockade is often given [10, 12]. Indeed, patients who have impaired ability to deploy immune cells or are lack of a balance between CD8⁺ T cells

and tumor burden responded weakly to immune checkpoint blockade therapies [13]. Thus, reinvigorating immune cells in tumors that are featured by high PD-L1 using type I interferon (IFN) could lead to proper T cell activation, a strategy that even could be employed as a combination with immune checkpoint blockades [14].

By deciphering the interplay among PD-L1, IFNs, and T cell function, studies have demonstrated that type I IFN signaling is indispensable for rejection of tumor cells via the initiation of anti-tumor T cell responses [15, 16]. Moreover, PD-L1 expression is mainly determined by IFNs, subsequently impairing the ability of T cells to eradicate tumor cells. However, the expression of type I IFNs in the tumor microenvironment is limited [14]. Indeed, the efficacy of conventional chemotherapeutics [17], targeted therapies [18], radiotherapy [19, 20], and immunotherapy [21, 22] could rely upon the induction of type I IFN signaling. As such, exogenous IFN α administration has been attempted to treat various tumor types, however, its short half-life and collateral toxicity restrict its clinical applications [23, 24]. Therefore, remodeling tumor microenvironment by reinforcing sustained type I IFN signals may be a feasible way to enhance immune checkpoint therapy responsiveness.

In this study, we used several tumor models to define the role of IFN α -MSCs in defending spontaneous tumors and eradicating established tumors in mouse models. We found that IFN α -MSC administration greatly inhibited tumor progression through enhancing the recruitment of CD8⁺ T cells and their cytotoxicity. Interestingly, such suppression is far-ranging and tumor specific. We found that IFN α -MSCs induced enriched CXCL10 expression in

¹CAS Key Laboratory of Tissue Microenvironment and Tumor, Shanghai Institute of Nutrition and Health, University of Chinese Academy of Sciences, Chinese Academy of Sciences, Shanghai 200031, China. ²The Third Affiliated Hospital of Soochow University, State Key Laboratory of Radiation Medicine and Protection, Institutes for Translational Medicine, Soochow University Medical College, Suzhou, Jiangsu 215123, China. ✉email: yufangshi@sibs.ac.cn; yingwang@sibs.ac.cn

Received: 10 August 2021 Revised: 22 December 2021 Accepted: 19 January 2022

Published online: 10 February 2022

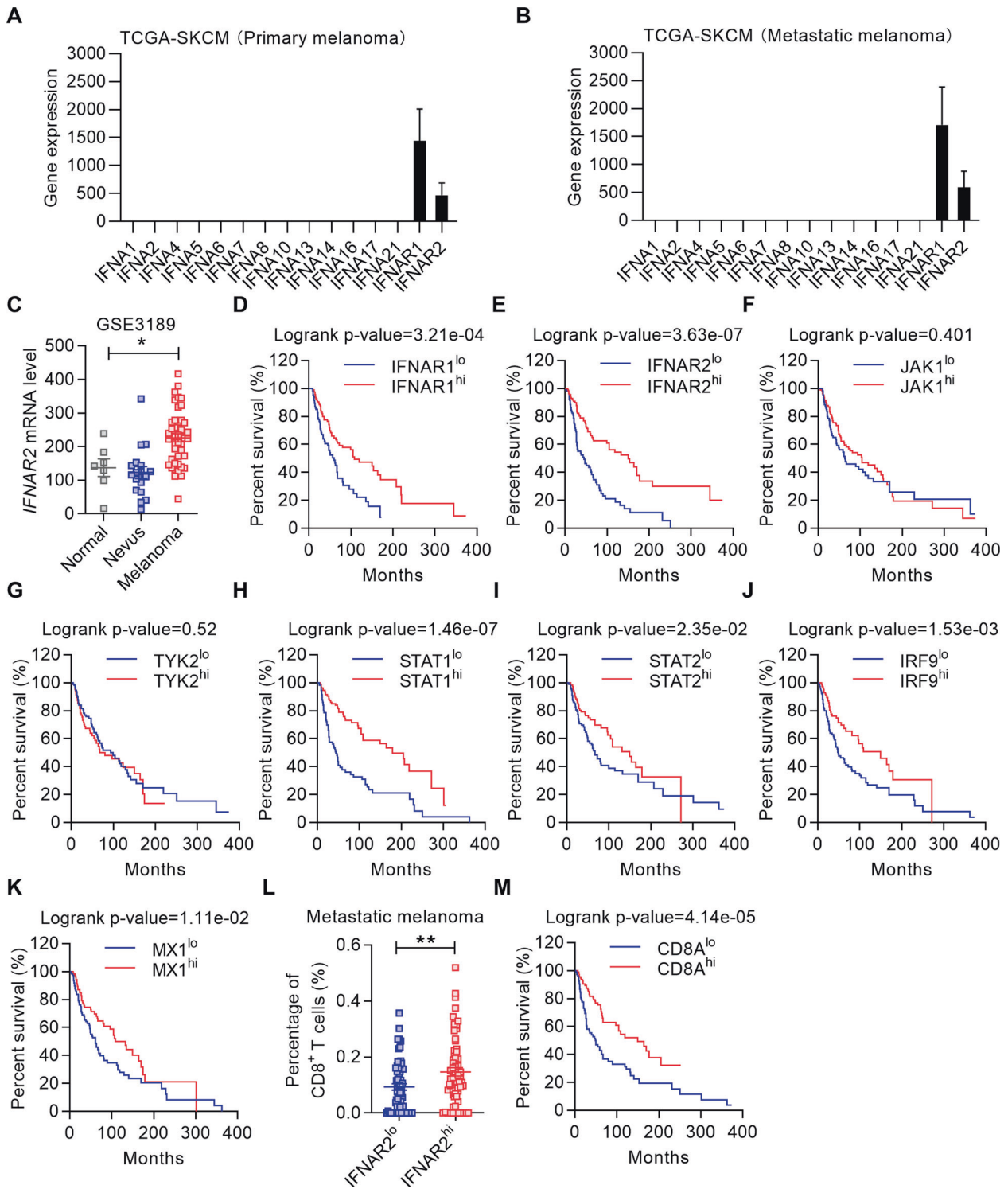
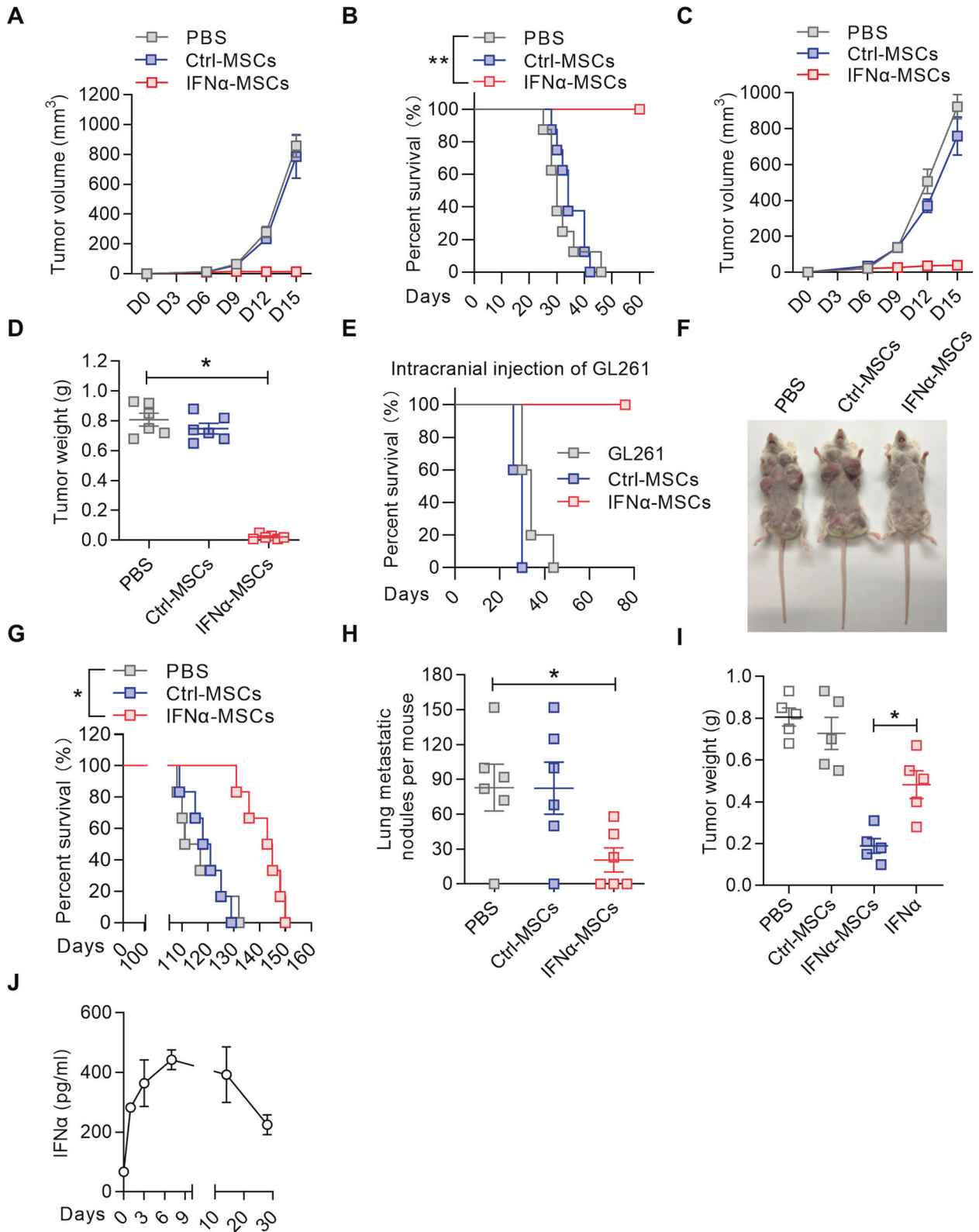


Fig. 1 Lack of type I IFN signaling is a negative prognostic indicator of melanoma patients. **A, B** The expressions of all *IFNA* subtypes and *IFNAR* in human primary melanoma (**A**) and metastatic melanoma (**B**). **C** Comparison of *IFNAR2* expression in normal skin, nevus, and melanoma tissues using the GSE3189 dataset. **D–K** The overall survival curves of patients with melanoma. Patients were stratified (cutoff at 25%) according to the expression of *IFNAR1* (**D**), *IFNAR2* (**E**), *JAK1* (**F**), *TYK2* (**G**), *STAT1* (**H**), *STAT2* (**I**), *IRF9* (**J**) and *MX1* (**K**) in the TCGA-SKCM dataset. **L** The percentages of $CD8^+$ T cells in patients with metastatic melanoma classified according to the expression of *IFNAR2*. Patients were stratified into *IFNAR2*^{lo} and *IFNAR2*^{hi} cohorts (cutoff at 25%). The percentages of $CD8^+$ T cells in the metastatic melanoma tissues were enumerated using CIBERSORT. **M** The overall survival analysis of melanoma patients with *CD8A*^{lo} and *CD8A*^{hi} expression (cutoff at 25%). Data are shown as means \pm SEM. * $p < 0.05$ and ** $p < 0.01$.

tumor cells which is responsible for the chemotaxis of $CD8^+$ T cells to the tumor site. IFN α derived from IFN α -MSCs increased the expression of GZMB in $CD8^+$ T cells through Stat3 signaling. Such concerted actions induced by IFN α -MSCs reinvigorated anti-tumor

response of $CD8^+$ T cells. More importantly, IFN α -MSCs, in combination with α -PD-L1 optimize the activation of $CD8^+$ T cells to control tumor. These findings may have important implications for developing more effective anti-tumor immunotherapies.



RESULTS

Low level of type I IFN signaling is associated with poor prognosis of melanoma

To investigate the correlation between type I IFN signaling and melanoma development, we used the Cancer Genome Atlas (TCGA) to analyze the expression patterns of *IFNA* and *IFNA*

receptor (*IFNAR*) in melanoma patients. Although all the *IFNA* transcripts were barely detectable, high levels of *IFNAR1* and *IFNAR2* expression were observed in both primary and metastatic melanoma (Fig. 1A, B and Supplementary Fig. S1A, B). We further compared the expressions of *IFNAR1* and *IFNAR2* in normal skins, nevus tissues, and melanoma tissues using a published dataset

Fig. 2 IFN α -MSCs elicit powerful anti-tumor activity. **A** Impact of IFN α -MSCs on B16F0 melanoma progression. B16F0 cells (1.0×10^6) were intramuscularly injected into the right outer thigh of mice. Mice received Ctrl-MSCs (1.0×10^6) or IFN α -MSCs (1.0×10^6) every 3 days starting on day 3. On days 6, 9, 12, and 15, tumor size was measured. **B** The survival curves of B16F0 melanoma bearing mice treated with PBS, MSCs, or IFN α -MSCs ($n = 8$). **C** Impact of IFN α -MSCs on MC38 tumor progression. Mice were intramuscularly injected with MC38 cells (1.0×10^6) and treated with Ctrl-MSCs (1.0×10^6) or IFN α -MSCs (1.0×10^6) every 3 days starting on day 3. On days 9, 12, and 15, tumor size was measured. **D** Mass of MC38 tumors treated with PBS, Ctrl-MSCs, or IFN α -MSCs ($n = 6$). **E** Impact of IFN α -MSCs on the survival of mice bearing GL261 tumors. Mice were intracranially co-injected with GL261 cells (2×10^5) and Ctrl-MSCs or IFN α -MSCs at a ratio of 300:1 ($n = 5$). **F** Visualization of tumor burden in MMTV-PyMT mice treated with PBS, Ctrl-MSCs, or IFN α -MSCs. MMTV-PyMT mice at 4 weeks old received Ctrl-MSCs (3.0×10^5) or IFN α -MSCs (3.0×10^5) twice a week. **G** The impact of IFN α -MSCs on the survival of MMTV-PyMT mice ($n = 6$). Data were pooled from two independent experiments. **H** The number of metastatic tumor nodules in the lungs of MMTV-PyMT mice treated with PBS, Ctrl-MSCs, or IFN α -MSCs ($n = 6$). **I** Comparison of the therapeutic effect of IFN α -MSCs and IFN α on melanoma. Mice were intramuscularly injected with B16F0 cells (1.0×10^6) and received single dose of Ctrl-MSCs (1.0×10^6), IFN α -MSCs (1.0×10^6), or IFN α (5 μ g) on day 5. The tumors were weighed on day 14 ($n = 5$). **J** IFN α concentration in the serum of melanoma bearing mice treated with IFN α -MSCs. Mice were co-injected with B16F0 cells (1.0×10^6) and IFN α -MSCs (1.0×10^6). IFN α in the serum was assayed at indicated times by ELISA. Data are presented as means \pm SEM. * $p < 0.05$ and ** $p < 0.01$.

(GSE3189) and found that the expressions of *IFNAR1* and *IFNAR2* are significantly higher in melanoma as compared to normal skin and nevus tissues (Fig. 1C and Supplementary Fig. S1C) [25]. These observations suggest that the alterations of *IFNAR* expression may modulate melanoma progression.

Distinct from janus kinase 1 (*JAK1*) and tyrosine kinase 2 (*TYK2*), the abundance of *IFNAR1*, *IFNAR2*, signal transducer and activator of transcription 1 (*STAT1*), signal transducer and activator of transcription 2 (*STAT2*), interferon regulatory factor 9 (*IRF9*), and MX dynamin-like GTPase 1 (*MX1*) are predictors of good prognosis of melanoma (Fig. 1D–K). Since all these genes were related to type I IFN activities, we employed cell-type identification by estimating relative subsets of RNA transcripts (CIBERSORT) algorithm to link the expression of *IFNAR* to CD8⁺ T cell infiltration [26]. We found that the expression of *IFNAR2*, but not *IFNAR1*, is correlated with the enrichment of infiltrated CD8⁺ T cells in the metastatic melanoma tissue microenvironment (Fig. 1L and Supplementary Fig. S1D). Patients with high expression of *CD8A* in the tumor site exhibited a higher overall survival rate (Fig. 1M). Taken together, these data demonstrate that type I IFN signatures in the tumor microenvironment predict a good prognosis of melanoma.

IFN α -MSCs elicit anti-tumor activities to several tumor types

Given a desert signature of type I IFN in the microenvironment of melanoma, we brought IFN α to the tumor site by employing MSCs constitutively expressing IFN α (IFN α -MSCs) to treat mice with tumors. These MSCs continuously release IFN α locally and thus avoid the concentration fluctuations and associated side effects of systemic administration of IFN α [27, 28]. Using ELISA assay, we verified that IFN α -MSCs robustly produced IFN α in vitro (Supplementary Fig. S2A). We investigated the anti-tumor effects of these IFN α -MSCs in several tumor models in vivo. In a mouse melanoma model, B16F0 were intramuscularly injected into the right outer thigh of C57BL/6 mice. IFN α -MSCs or Ctrl-MSCs were locally injected into peritumoral tissue every 3 days starting on day 3 (Fig. 2A). We found that IFN α -MSCs completely inhibited melanoma growth. In comparison with PBS and Ctrl-MSC treatment, administration of IFN α -MSCs blocked tumor growth and dramatically prolonged the survival of mice bearing melanoma (Fig. 2B). We further utilized IFN α -MSCs to treat colon carcinoma established by the MC38 cell line and found that IFN α -MSCs also exerted a dramatic suppression on tumor growth as measured by tumor volume (Fig. 2C) and tumor weight (Fig. 2D). In a mouse glioma model, GL261 cells were intracranially injected together with Ctrl-MSCs or IFN α -MSCs at a ratio of 300:1. At the time point when all PBS and Ctrl-MSC treated mice reached the point to be euthanized, all mice received IFN α -MSC treatment remain alive (Fig. 2E). These results clearly demonstrate that IFN α -MSCs could exert powerful anti-tumor effect on tumor growth.

We further tested the therapeutic effect of IFN α -MSCs in the B16F10 melanoma model. B16F10 cells were *i.v.* injected into

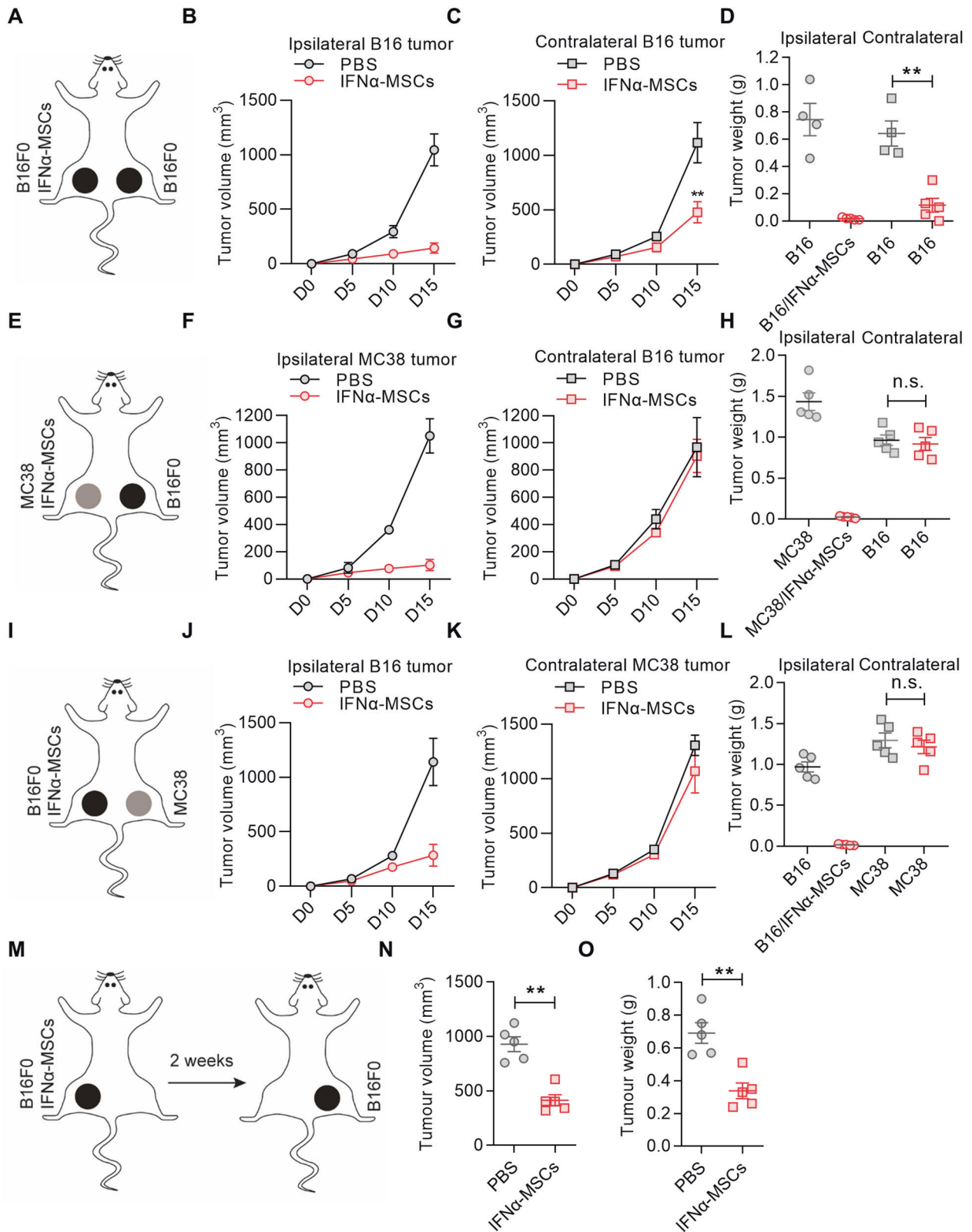
C57BL/6 mice. On day 7, these mice received a single dose of IFN α -MSC infusion. We found that IFN α -MSC treatment significantly inhibited B16F10 melanoma colonization in the lung (Supplementary Fig. S2B–D) and prolonged the survival of tumor bearing mice (Supplementary Fig. S2E). To extend our findings to spontaneously developed tumors, we used IFN α -MSCs to treat MMTV-PyMT mice, which develop spontaneous mammary tumors. At 4 weeks old, the MMTV-PyMT mice were *i.v.* administered with PBS, Ctrl-MSCs, or IFN α -MSCs twice a week. IFN α -MSC administration dramatically decreased the tumor burden of MMTV-PyMT mice and extended their survival (Fig. 2F, G), suggesting a robust anti-tumor effect of IFN α -MSCs. This was consolidated by the observation that IFN α -MSC administration also resulted in a dramatic reduction of tumor metastasis to the lungs (Fig. 2H).

As IFN α has been approved for treating several neoplasms, we compared the anti-tumor effects of IFN α and IFN α -MSCs, and found that IFN α -MSCs exhibited a much more powerful suppression on tumor growth than that of intra-tumoral injection of IFN α (Fig. 2I). By monitoring the serum level of IFN α in IFN α -MSC-treated mice, we found that administration of IFN α -MSCs could sustainably elevate IFN α level in the serum, even on day 28 (Fig. 2J). Distinct from the flu-like symptoms induced by IFN α , IFN α -MSC treatment has no influence on mouse body weight, temperature, and leukocyte number in blood (Supplementary Fig. S2F–H). Therefore, IFN α -MSCs exert extensive anti-tumor effects with no noticeable toxicity.

IFN α -MSCs impose tumor specific abscopal anti-tumor effect

To investigate the mechanism(s) underlying the tumoricidal effect of IFN α -MSCs, we firstly used their conditioned medium to treat B16F0 cells. Although the conditioned medium of IFN α -MSCs slightly suppressed the tumor growth in vitro, such inhibitory effect may not be the major reason to suppress tumor in vivo (Supplementary Fig. S3A). Consistently, we found that IFN α , even at very high dose, has very limited effects on tumor growth (Supplementary Fig. S3B). Furthermore, no significant influence on cell cycle and apoptosis was observed in B16F0 cells treated with IFN α or conditioned medium of IFN α -MSCs (Supplementary Fig. S3C, D). Thus, the anti-tumor activities of IFN α -MSCs are independent of the direct killing effect of IFN α on tumor cells.

We then examined whether local administration of IFN α -MSCs could initiate systemic anti-tumor immunity. To this end, a mouse bilateral tumor model in which B16F0 cells were inoculated to both outer thighs was employed to evaluate the systemic tumoricidal effect of IFN α -MSCs (Fig. 3A). In this model, the left outer thigh of C57BL/6 mice was co-injected with B16F0 cells and IFN α -MSCs at a ratio of 1:1, while the right outer thigh only inoculated with B16F0 cells. Intriguingly, the introduction of IFN α -MSCs in the left outer thigh significantly inhibited tumor growth in the right outer thigh (Fig. 3B–D), suggesting an induction of a far-ranging anti-tumor immunity by IFN α -MSCs.



We next sought to determine whether the abscopal effect of the anti-tumor activity is tumor specific. B16F0 and antigenically distinct MC38 cells were separately injected in the outer thighs of mice (Fig. 3E). We found that co-administration of IFN α -MSCs with MC38 cells failed to inhibit the growth of B16F0 tumor (Fig. 3F–H). Likewise, co-injection of B16F0 cells with IFN α -MSCs was unable to

suppress MC38 tumor growth (Fig. 3I–L). Importantly, B16F0 cells co-injected with IFN α -MSCs in one thigh blocked the growth of B16F0 tumor on the opposite thigh that was induced at 2 weeks after tumor and IFN α -MSCs injection (Fig. 3M). Compared with counterparts, the tumor sizes and volumes were much smaller in IFN α -MSC-administrated mice, suggesting a long-lasting anti-

Fig. 3 IFN α -MSCs impose systemic specific anti-tumor effect. **A** Schematic representation of the impact of IFN α -MSCs on abscopal tumors. Mice received the co-injection of B16F0 cells (1.0×10^6) and IFN α -MSCs (1.0×10^6) in the left outer thigh and simultaneously inoculated with B16F0 cells (1.0×10^6) in the right outer thigh. **B, C** Tumor volumes of ipsilateral (**B**) and contralateral (**C**) B16 tumors treated with or without IFN α -MSCs. **D** Tumor weight of ipsilateral and contralateral B16 tumors treated with or without IFN α -MSCs ($n = 4$ or 5). **E** Schematic representation of the impact of IFN α -MSCs on abscopal B16F0 tumors. Mice received co-injection of MC38 cells (1.0×10^6) and IFN α -MSCs (1.0×10^6) in the left outer thigh, and B16F0 cells (1.0×10^6) only in the right outer thigh. Tumor sizes of both sides were measured. **F, G** Tumor volumes of ipsilateral MC38 tumors (**F**) and contralateral B16 tumors (**G**). **H** Tumor weights of ipsilateral MC38 tumors and contralateral B16 tumors ($n = 5$). **I** Schematic representation of the impact of IFN α -MSCs on abscopal MC38 tumor. B16F0 cells (1.0×10^5) with IFN α -MSCs (1.0×10^6) were co-injected intramuscularly into left outer thigh, then re-challenged with B16F0 cells (2.0×10^5) in right outer thigh 2 weeks later. **J** Tumor volumes of ipsilateral B16 tumors. **K** Tumor volumes of contralateral MC38 tumors. **L** Weights of ipsilateral B16 tumors and contralateral MC38 tumors ($n = 5$). **M** Schematic representation of the duration of the anti-tumor effect of IFN α -MSCs. Mice were co-injected intramuscularly with B16F0 cells (1.0×10^5) and IFN α -MSCs (1.0×10^6) in the left outer thigh. Two weeks later, mice were injected with B16F0 cells (2.0×10^5) in the right outer thigh. **N, O** Volumes (**N**) and weights (**O**) of B16 tumors in the right outer thigh ($n = 5$). Data are shown as means \pm SEM. * $p < 0.05$ and ** $p < 0.01$.

tumor effect (Fig. 3N, O). Taken together, the tumoricidal activity initiated by IFN α -MSCs can act remotely in a tumor specific and long-lasting manner.

CD8⁺ T cells are essential in mediating the anti-tumor effect of IFN α -MSCs

Given the specific effects of IFN α -MSCs on limiting remote tumors and the induction of T cell accumulation at the tumor site (Supplementary Fig. S4A), we verified whether T cells are involved in the anti-tumor effects of these cells. The anti-tumor effects of IFN α -MSCs were evaluated in Rag2^{-/-} mice. We found that IFN α -MSCs exhibited partial impairment in tumor growth in Rag2^{-/-} mice (77.7% vs 41.5%) (Fig. 4A and Supplementary Fig. S4B). To examine which T cell population is critical, we further employed mice deficiency in MHC class II trans-activator (*Ciita*) [29] and β 2-microglobulin (β 2m) [30]. In *Ciita*^{-/-} mice, IFN α -MSCs exhibited similar ability in restraining tumor growth as WT mice (Fig. 4B), suggesting that CD4⁺ T cells are dispensable for the anti-tumor effect of IFN α -MSCs. However, IFN α -MSCs cannot efficiently suppress tumor growth in β 2m^{-/-} mice (Fig. 4C), arguing the importance of CD8⁺ T cells. Antibody-mediated depletion of CD8⁺ T cells also attenuated the efficacy of IFN α -MSCs in suppressing tumor growth (Fig. 4D and Supplementary Fig. S4C). These data demonstrate that the anti-tumor effect of IFN α -MSCs mainly relies on CD8⁺ T cells.

Next, we profiled the immune cells in mice bearing B16F0 melanoma treated with or without IFN α -MSCs. The circulating and splenic T cells were not affected by IFN α -MSC administration (Fig. 4E and Supplementary Fig. S4D). However, the number and proportion of tumor infiltrated CD8⁺ T cells were dramatically increased in IFN α -MSCs treated mice (Fig. 4E–G). Moreover, CD8⁺ T cells in the tumor draining lymph node of mice treated with IFN α -MSCs exhibited a preference for the central memory phenotype (CD44⁺CD62L⁺) (Fig. 4H). By conducting Ki67 staining in intra-tumoral CD8⁺ T cells, we excluded the direct influence of IFN α -MSCs on T cell proliferation (Fig. 4I). Interestingly, when we utilized FTY720, a sphingosine 1-phosphate (S1P) receptor agonist, to block the egress of lymphocytes from lymphoid organs (Supplementary Fig. S4E), we found that the inhibition of IFN α -MSCs on tumor growth were dramatically impaired (Fig. 4J). Taken together, these results demonstrate that IFN α -MSCs facilitate the infiltration of CD8⁺ T cells in tumors, and thus lead to the suppression on tumor growth.

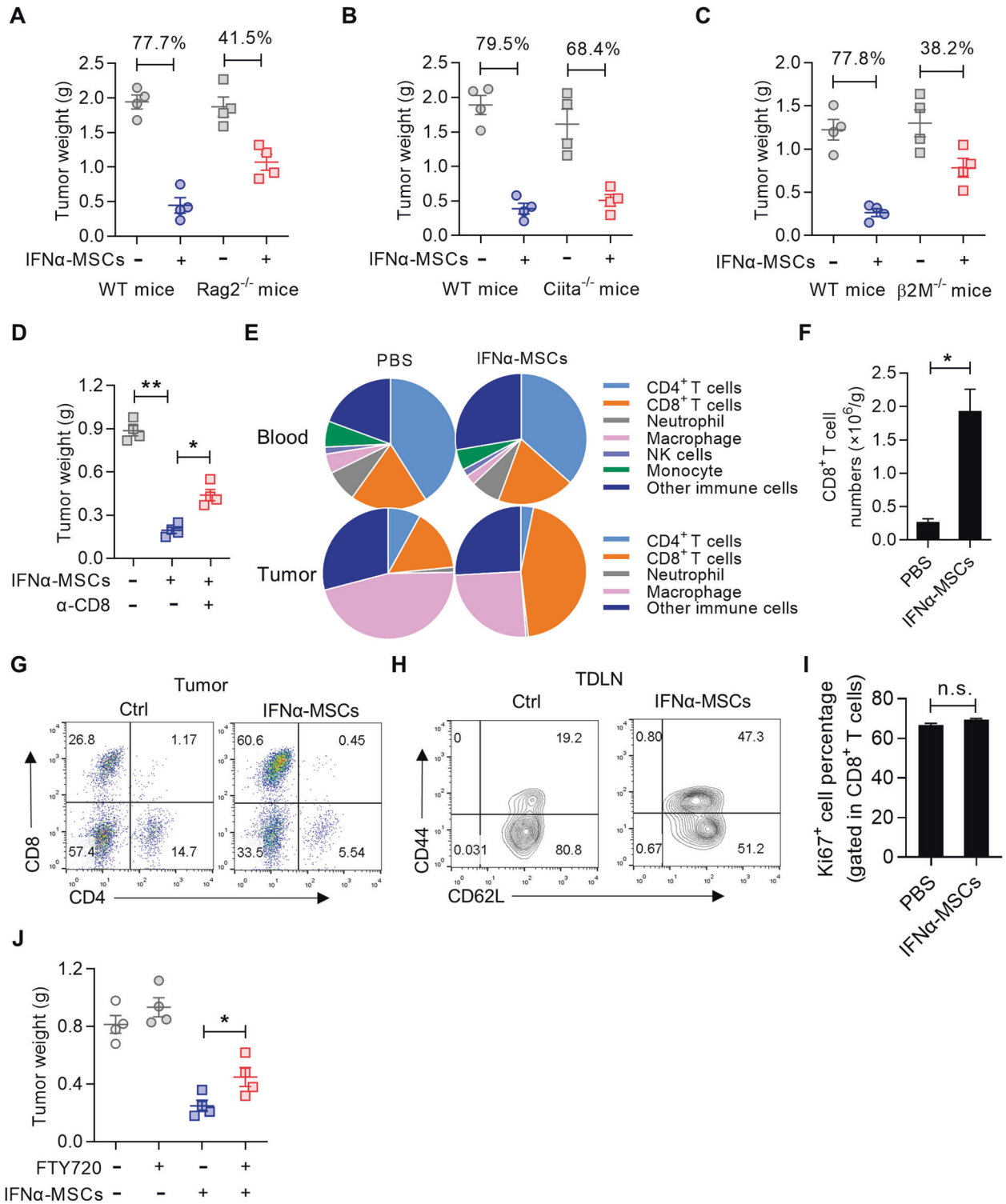
IFN α -MSCs enhance CD8⁺ T cell infiltration into tumor via the CXCL10-CXCR3 axis

To investigate the molecular mechanism(s) of IFN α -MSC-facilitated CD8⁺ T cell infiltration into tumors, we examined the chemokine expression profiles in matched tumor tissues. Compared to the control group, intra-tumoral injection of IFN α -MSCs upregulated the expressions of *Ccl3*, *Ccl4*, *Ccl5*, *Cxcl10*, *Cxcl11*, and *Cxcl12* in tumors (Fig. 5A). Among them, *Cxcl9*, *Cxcl10*, and *Cxcl11* are most

related to the recruitment of CD8⁺ T cells, as CXCR3, the cognate receptor for CXCL9 and CXCL10, is highly expressed in tumor infiltrated CD8⁺ T cells (Supplementary Fig. S5A). To distinguish the main source of these chemokines, we detected the expression of chemokines in B16F0 cells, IFN α -treated B16F0 cells, Ctrl-MSCs, IFN α -MSCs, CD45⁺ cells, and CD45⁺ cells treated with IFN α by qPCR (Fig. 5B). A significantly higher levels of CXCR3 ligands, *Cxcl9* and *Cxcl10*, were observed in B16F0 cells stimulated with IFN α , but lower in Ctrl-MSCs or IFN α -MSCs (Supplementary Fig. S5B–D). Of note, only *Cxcl10* was highly expressed in B16F0 cells (Supplementary Fig. S5E). Given that an inverted relation between the tumor weight and CD8⁺ T cell infiltration and a dramatic downregulation of *Cxcl10* in melanoma at the late stage (Fig. 5C, D), we tested if addition of IFN α or IFN α -MSCs could enhance the expression of CXCL10 in B16F0 cells. Indeed, a significant enhancement of CXCL10 was observed in B16F0 cells treated with conditional medium of IFN α -MSCs, to a comparable level of that in IFN α treated B16F0 cells (Fig. 5E). Furthermore, IFN α -MSC administration elevated the concentration of CXCL10 in tumors (Fig. 5F).

By employing a transwell assay, we verified the role of CXCL10 in mediating CD8⁺ T cell migration via CXCR3 (Fig. 5G and Supplementary Fig. S5F). Additionally, we engineered B16F0 cells with *Cxcl10* knockdown (shCxl10) or *Cxcl10* overexpression (OE-Cxl10) using lentivirus transfection. We found that shCxl10 B16F0 cell culture medium diminished, while OE-Cxl10 B16F0 cell culture medium promoted CD8⁺ T cell migration (Fig. 5H). When compared with control B16F0 tumor, shCxl10 B16F0 tumor showed compromised response to IFN α -MSC treatment in vivo (Fig. 5I). Consistently, knockdown of *Cxcl10* in B16F0 cells impaired IFN α -MSC-induced CD8⁺ T cell infiltration into tumor (Fig. 5J). We also found that primary melanoma or metastatic melanoma patients with higher levels of CXCL10 expression exhibited more CD8⁺ T cell infiltration (Fig. 5K, L). In addition, high expression of CXCL10 in patients suffering melanoma is an indicator of a good prognosis (Fig. 5M). These data strongly argue that melanoma cells can be influenced by IFN α released from IFN α -MSCs to produce CXCL10 to recruit CD8⁺ T cells into tumors.

We then investigated the molecular mechanisms that are involved in IFN α inducing CXCL10 expression. It has been reported that the NF- κ B signaling pathway regulates CXCL10 expression [31]. However, using NF- κ B inhibitor (PDTC) or IKK inhibitor (BAY 11-7082) to treat B16F0 cells showed little influence on IFN α -induced *Cxcl10* expression (Supplementary Fig. S5G). We next tested whether transducers and activators of transcription (Stats) in B16F0 cells mediate IFN α -induced CXCL10 expression. To achieve this, we used inhibitors (Fludarabine and Stattic) to block Stat1 and Stat3, respectively. We found that Stat1, but not Stat3, mediates CXCL10 expression induced by IFN α in B16F0 cells (Fig. 5N, O and Supplementary Fig. S5H). Together, IFN α -MSCs act on B16F0 cells and drive CD8⁺ T cell accumulation in the tumor through the IFN α -Stat1-CXCL10-CXCR3 axis.



IFNα-MSCs potentiate the cytotoxicity of CD8⁺ T cells via the Stat3 signaling

Given the key role of CD8⁺ T cells in eradicating tumor cells, we sought to test the direct effect of IFNα on CD8⁺ T cells. Upon activation by anti-CD3 and anti-CD28, the addition of IFNα enhanced the expressions of CD25 and CD69 on CD8⁺ T cells, but no obvious influence on their proliferation (Supplementary Fig. S6A–C). To gain further insights into the mechanism(s) underlying how IFNα regulates CD8⁺ T cell function, we

performed RNA-seq in CD8⁺ T cells with or without IFNα stimulation. IFNα imposed a distinct gene expression pattern on CD8⁺ T cells (Fig. 6A). Gene ontology analysis showed that the upregulated gene signature in IFNα treated CD8⁺ T cells was predominantly enriched for transcripts associated with “responses to virus”, “cellular responses to type I IFN” and “defense responses to virus” (Fig. 6B). Consistently, pathways related to “virus infection” and “immune response” were changed prominently upon IFNα treatment (Supplementary Fig. S6D). The heatmap data

Fig. 4 **CD8⁺ T cells are essential for the anti-tumor effect of IFN α -MSCs.** **A–C** The impact of IFN α -MSCs on tumor growth in immunodeficient mice. B16F0 cells were intramuscularly injected into wild type (WT), Rag2^{-/-} (A), Ctiita^{-/-} (B), or β 2m^{-/-} mice (C). On day 5, mice were *i.m.* injected with IFN α -MSCs (1.0×10^6). On day 18, tumor weight was determined ($n = 4$). **D** The influence of depletion of CD8⁺ T cells on the anti-tumor effect of IFN α -MSCs. Mice were *i.m.* injected with B16F0 cells and administrated with IFN α -MSCs (1.0×10^6), CD8 depleting Ab (α -CD8, clone number 2.43), or both. On day 18, tumor weight was determined ($n = 4$). **E** Profiling of immune cells in tumors and blood of tumor bearing mice with or without IFN α -MSC administration. On day 5, mice were *i.m.* injected with IFN α -MSCs (1.0×10^6). On day 18, blood and tumor tissue were harvested for flow cytometric analysis. Shown are results of two independently experiments. **F** Numbers of tumor infiltrated CD8⁺ T cells in tumor bearing mice with or without IFN α -MSC administration. **G** Ratio of CD4⁺ and CD8⁺ T cells in tumors of mice with or without IFN α -MSC administration. **H** Expressions of CD44 and CD62L on CD8⁺ T cells in draining lymph node (TDLN) of tumor bearing mice with or without IFN α -MSC administration. **I** Expression of Ki67 in intra-tumoral CD8⁺ T cells of mice treated with or without IFN α -MSC administration. **J** The influence of blocking the egress of CD8⁺ T cells on the anti-tumor effect of IFN α -MSCs. Mice were intramuscularly injected with B16F0 cells and administrated with IFN α -MSCs (1.0×10^6), FTY720 (1 mg/kg every 2 days) or both. On day 18, tumor weight was determined ($n = 4$). Data are shown as means \pm SEM. n.s., no significance, * $p < 0.05$ and ** $p < 0.01$.

showed that IFN α treatment sharply increased the expression of Granzyme B (*Gzmb*), a gene signature for the cytotoxicity of CD8⁺ T cells (Fig. 6C). In line with this, IFN α or condition medium of IFN α -MSCs markedly promoted *Gzmb* expression (Fig. 6D and Supplementary Fig. S6E). Accordingly, administration of IFN α -MSCs to mice bearing B16F0 cells could dramatically promote the expression of GZMB in tumor infiltrated CD8⁺ T cells (Fig. 6E, F). In addition, these tumor infiltrated CD8⁺ T cells treated with IFN α exhibited stronger tumoricidal activity than those in mice of the control group (Fig. 6G).

We also investigated whether Stat(s) would be able to control the expression of GZMB in CD8⁺ T cells upon IFN α stimulation. Indeed, enhanced phosphorylation of Stat3 at Tyr705 was observed in IFN α treated CD8⁺ T cells, and this effect was markedly compromised by Stattic treatment (Fig. 6H, I). Both Stat1 inhibitor (Fludarabine) and Stat3 inhibitor (Stattic) were used to treat CD8⁺ T cells, in the presence or absence of IFN α . We found that IFN α -induced *Gzmb* expression is mediated by Stat3, but not Stat1 (Fig. 6H and Supplementary Fig. S6F). We further employed the Cre/Loxp system to specifically delete Stat3 in T cells *in vivo*. Compared to CD8⁺ T cells derived from Stat3^{fl/fl} mice, CD8⁺ T cells isolated from CD8^{Cre}Stat3^{fl/fl} mice expressed lower level of *Gzmb*. Moreover, IFN α -induced *Gzmb* expression was impaired in CD8⁺ T cells with Stat3 deletion (Fig. 6J). By analysis of SKCM-TCGA data, we also found a positive correlation between *STAT3* and *GZMB* expression in human melanoma (Supplementary Fig. S6G). Consistently, melanoma patients with higher level expression of *STAT3* or *GZMB* suggested a good prognosis (Fig. 6K, L). Therefore, these data demonstrate that the release of IFN α by IFN α -MSCs reinforces the cytotoxicity of CD8⁺ T cells via regulation of the Stat3 signaling.

IFN α -MSCs improve the efficacy of PD-L1 blockade

Lack of preexisting immune cell infiltration is an indicator of primary resistance to immune checkpoint blockade [32]. Given the powerful ability of IFN α -MSCs in deployment of CD8⁺ T cells into tumors, we hypothesized that combination of IFN α -MSCs and PD-L1 blockade may modulate the immune context of tumor and empower more potent anti-tumor effect. This notion is supported by the analysis of RNA sequencing data from PD-1 responders and non-responders, which showed that both *IFNA* and *IFNARs* were expressed at higher levels in patients responded well to the treatment of PD-1 blockade (Fig. 7A) [33]. Patients that respond to PD-1 blockade also exhibited increased expression of *STAT1*, *CXCL9*, *CXCL10*, *GZMB*, *CD8A*, and *CD8B*, which is consistent with our observation in tumor model with IFN α -MSC treatment (Fig. 7B). We re-analyzed their immunohistochemistry data and found that the density of CD3⁺, CD4⁺, and CD8⁺ T cells were prominently higher in anti-PD1 responders as compared to non-responders (Fig. 7C).

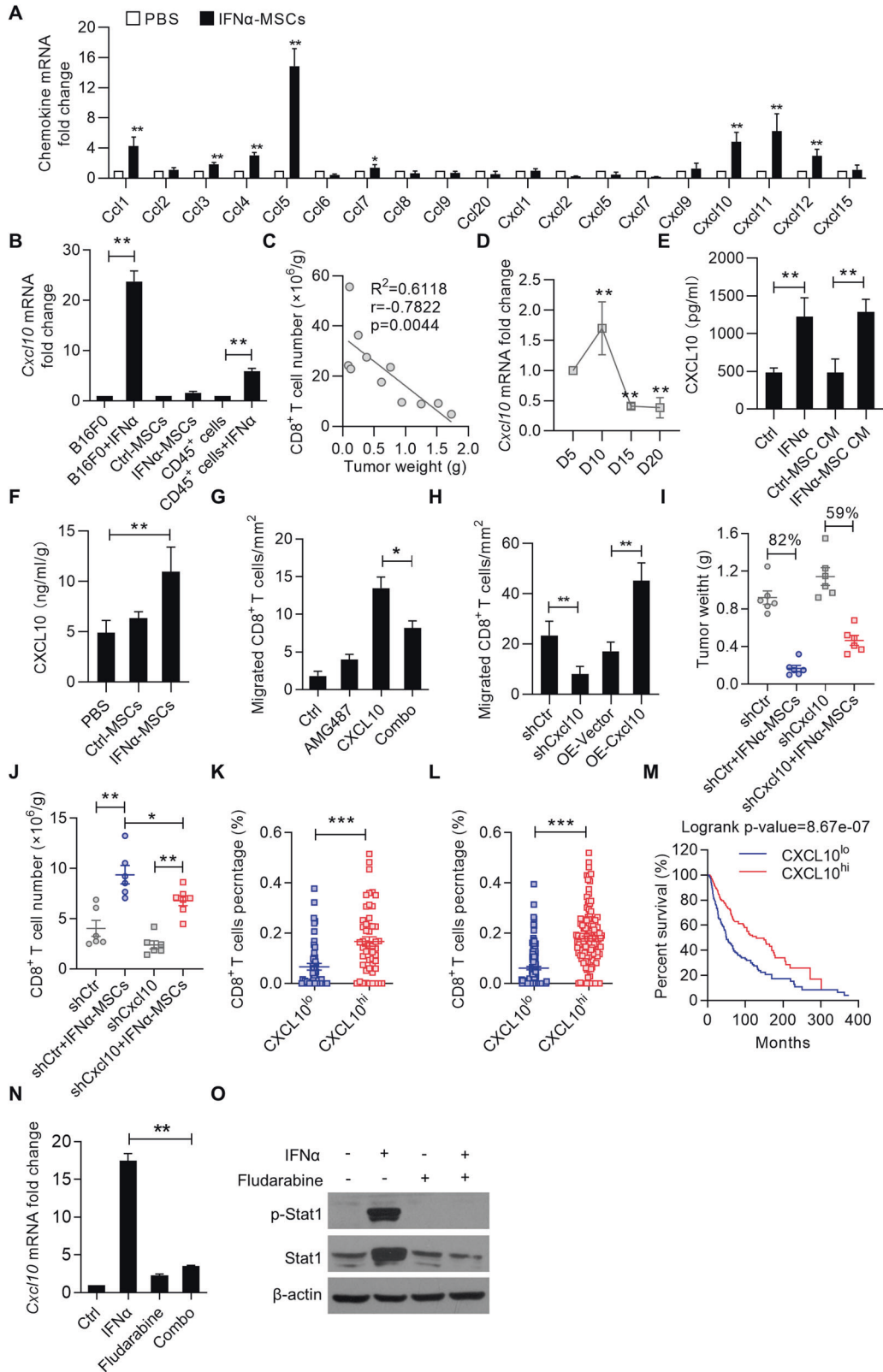
IFN α is one of the most potent inducers of PD-L1, which serves as a negative feedback mechanism to dampen immune responses [34]. Consistent with previous studies, we found that IFN α robustly

induce PD-L1 expression in a dose-dependent manner in B16F0 cells (Supplementary Fig. S7A, B). In the mouse melanoma model, however, α -PD-L1 alone administration only had minor impact on the rate of tumor growth, suggesting simple blockade of the immune checkpoint is insufficient to elicit a powerful anti-tumor immune response. However, in comparison with the control group, mouse treated with the combination of IFN α -MSCs and α -PD-L1 profoundly decreased tumor growth (Fig. 7D, E) and increased survival time of tumor bearing mice over monotherapies (Fig. 7F). To better understand how the treatment with α -PD-L1 plus IFN α -MSC regulated the tumor immune response, we counted CD8⁺ T cells in matched tumors. Treatment with IFN α -MSCs and α -PD-L1 significantly increased CD8⁺ T cells in tumor (Fig. 7G). To further verify whether CD8⁺ T cells are responsible for the enhancement of anti-tumor efficacy of α -PD-L1 plus IFN α -MSCs, we depleted CD8⁺ T cells by intraperitoneal injection α -CD8 antibody (clone number 2.43). Depletion of CD8⁺ T cells diminished the anti-tumor effects of α -PD-L1 plus IFN α -MSCs, but had no effect in the untreated group (Fig. 7H). Moreover, the survival benefit induced by the combination treatment was comprised when CD8⁺ T cells were depleted (Fig. 7I). Collectively, these results indicate that administration IFN α -MSCs could strikingly enhance the responsiveness to PD-L1 blockade.

DISCUSSION

The paucity of immune cells in tumors adversely correlates with patient prognosis. Remodeling tumor microenvironment holds great promise for cancer treatment. Here, we found that administration of IFN α -MSCs attracted CD8⁺ T cells into tumors and elicited anti-tumor activities. In the tumor microenvironment, IFN α -MSCs suppress tumor progression in an action of “killing two birds with one stone”: (i) Promoting CD8⁺ T cell infiltration into tumor tissue; (ii) Potentiating the cytotoxicity of CD8⁺ T cells in a tumor specific manner (Fig. 8). Of note, combination treatment of IFN α -MSCs and PD-L1 blockade synergistically suppresses tumor growth and significantly improves the survival of tumor bearing mice.

Consistent with previous studies, our analysis demonstrated that low levels of signals elicited by type I IFNs correlate with poor prognosis in melanoma patients. Therefore, reintroduction of type I IFNs or IFN signaling are principally important in combating tumor [35]. However, systemic administration of type I IFNs is always accompanied by severe adverse effects, limiting their clinical applications. In our previous studies, we equipped MSCs with IFN α and tested their ability to specifically deliver IFN α to solid tumors [27, 28]. Compared to IFN α , IFN α -MSCs were more effective in suppression of tumor growth. More importantly, IFN α -MSCs remodel anti-tumor immune microenvironment through a concerted action. In this scenario, IFN α -MSCs in tumor sites induce the production of CXCL10 in tumor cells which in turn mobilizes CD8⁺ T cell into tumors. Meanwhile, IFN α released by IFN α -MSCs enhances the expression of GZMB in CD8⁺ T cells and thus



promotes their ability to eradicate tumor cells. Therefore, employment of IFN α -MSCs to modulate tumor microenvironment holds great promise in the treatment of solid tumors.

Clinically, primary tumors have more optional treatments, including surgery, chemotherapy, radiotherapy, and immunotherapy. However, the available treatments for unresectable or drug-resistant

tumors are largely limited [36]. In fact, about >90% of mortality from cancer is attributable to subsequent metastases [37]. Thus, there is a desperate need to develop novel strategy to target local and distant tumors concurrently. In this study, by employing bilateral tumor model, we found that introduction of IFN α -MSCs in ipsilateral tumors could control the growth of contralateral tumors. Evidence that local

Fig. 5 IFN α -MSCs enhance CD8⁺ T cell infiltration into tumors via the CXCL10-CXCR3 axis. **A** The chemokine expression profile in tumors of mice with or without IFN α -MSC treatment. **B** Expressions of *Cxcl10* in B16F0 cells, IFN α treated B16F0 cells, Ctrl-MSCs, IFN α -MSCs, CD45⁺ cells, and CD45⁺ cells treated with IFN α . **C** Scatterplots showing the correlation between the number of CD8⁺ T cells and tumor weight ($n = 11$). **D** The expression of *Cxcl10* in B16F0 tumors at indicated times. **E** Level of CXCL10 produced by B16F0 cells treated with IFN α , condition medium (CM) of Ctrl-MSCs or IFN α -MSCs. Level of CXCL10 was assessed by ELISA. **F** Level of CXCL10 in tumors of mice treated with Ctrl-MSCs or IFN α -MSCs. **G** Chemotaxis of CD8⁺ T cells in response to CXCL10. Naïve CD8⁺ T cells isolated from mouse spleen were stimulated by anti-CD3 and anti-CD28 for 48 h. Then, the migration of CD8⁺ T cells was assessed by the transwell system in the presence of CXCL10 (1 μ g/ml), AMG487 (1 μ M) or both for 4 h. **H** Chemotaxis of CD8⁺ T cells in response to the condition medium of B16F0 with *Cxcl10* knockdown or overexpression. B16F0 cells were transduced with lentivirus carrying *Cxcl10* shRNA or vector for gene encoding *Cxcl10*. Supernatant was obtained and used to test the impact on CD8⁺ T cell migration by transwell assay. OE, overexpression. **I** Tumor mass. Mice were inoculated with shCtrl and sh*Cxcl10* B16F0 cells and administered with IFN α -MSCs (1.0 \times 10⁶ per mouse, *i.m.*) on day 5. **J** Numbers of CD8⁺ T cells in the tumor of mice inoculated with shCtrl and sh*Cxcl10* B16F0 cells and treated with IFN α -MSCs. **K, L** Comparison of the percentage of CD8⁺ T cells in melanoma between the CXCL10 low (CXCL10^{lo}) and CXCL10 high (CXCL10^{hi}) groups. Primary (K) and metastatic (L) melanoma patients based on CXCL10 expression were stratified into CXCL10^{lo} and CXCL10^{hi} cohorts (cutoff at 25%). The percentage of CD8⁺ T cells in melanoma were enumerated using CIBERSORT. **M** The overall survival analysis in CXCL10^{lo} and CXCL10^{hi} melanoma patients (cutoff at 25%). **N, O** Expression of *Cxcl10* (N) and Stat1 phosphorylation (O) in B16F0 cells treated with IFN α (1000 U/ml), Fludarabine (50 μ M), or both. Data are shown as means \pm SEM. * $p < 0.05$, ** $p < 0.01$ and *** $p < 0.001$.

administration of IFN α -MSCs contributed to a systemic anti-tumor effect was provided by the increase in CD44⁺CD62L⁺CD8⁺ T cells in tumor draining lymph node observed in tumors injected with IFN α -MSCs. Therefore, administration of IFN α -MSCs may be an ideal therapeutic strategy to treat cancer patients with distal metastases.

Our study provides further insights into anti-tumor immunotherapies. A combination therapy of IFN α -MSCs and PD-L1 blockade demonstrated an enhancement in survival and tumor control. Such a combination reversed the paucity of immune cell infiltration in the tumor microenvironment, a major reason for the failure of immune checkpoint blockade treatment. Previous studies have demonstrated that promoting the infiltration of tumor antigen-specific CD8⁺ T cells in tumors can strengthen immunotherapy response [38, 39]. Activation of type I IFN signaling improved the efficacy of PD-1 blockade in melanoma featured by less immune cells [40]. Consistently, type I IFN fusion protein could optimize the therapeutic effects of PD-L1 blockade [14, 18, 41]. Together, these findings consolidate that targeted delivery of type I IFN into the tumor microenvironment is a feasible approach to enhance the therapeutic effect of immune checkpoint blockade treatment. Future investigations should be focused on exploring whether IFN α -MSC administration could optimize the efficacies of other anti-tumor strategies, such as tumor vaccination, radiotherapy, and chemotherapy [42–44].

IFN α treatment facilitates lymphocyte infiltration into tumors through augment of CXCL10 production by tumor cells. CXCR3, a receptor for CXCL9, CXCL10, and CXCL11, is expressed on T cells [45]. Activation of CXCR3 could induce T cell infiltration into inflamed sites [46]. However, CXCR3 is also expressed on melanoma cells. It has been reported that ligation with CXCL10 increased the metastasis of melanoma [47–49]. Therefore, strategies targeting CXCR3 to boost cytotoxic T lymphocyte recruitment should be carefully designed to avoid the hijack of melanoma cells.

It should be noted that type I IFNs have dramatic effects on the activation, migration, differentiation, function, and survival of innate immune cells, including dendritic cells, natural killer cells, macrophages, neutrophils, and monocytes [16, 50–55]. Type I IFNs stimulated antigen presenting cells to express high levels of MHC molecules and co-stimulatory molecules, such as CD80 and CD86 [56], which are critical in initiating and amplifying T cell activation. A recent publication also emphasized that delivery of type I interferon elicited an anti-tumor immunity via XCR1⁺ dendritic cells [51]. Therefore, the influence of IFN α produced by IFN α -MSCs on CD8⁺ T cells could involve its regulation on innate immune cells. Future investigation will examine the roles of dendritic cells and macrophages in the anti-tumor T cell immunity induced by IFN α -MSCs. In addition, MSCs are well-known in immunosuppression, raising the

potential in orchestrating tumor immune microenvironment to facilitate tumor progression. In fact, the immunosuppression of MSCs should be evoked by IFN γ and TNF or IL-1 and can be totally abolished by the presence of IFN α [28]. We here demonstrate that MSCs equipped with IFN α can deploy tumoricidal CD8⁺ T cells in tumor microenvironment and synergistically enhance anti-tumor effect of α -PD-L1.

Together, our study highlights the potential to harness IFN α -MSCs to invigorate T cells and remodel tumor immune microenvironment, which should have beneficial effects in eradicating multiple types of tumors. Such approach provides insights into the application of immune checkpoint blockade, which need the preexisting T cell infiltration and/or presence of PD-L1 and PD-1. It is critical to examine if the strategies reported herein can be extended to other tumor types, especially those that are less immunogenic. Nevertheless, our study not only illustrates the molecular mechanism of the utilization of IFN α -MSCs in eradicating tumors, but also verifies an approach of using IFN α -MSCs to enhance the responsiveness to immune checkpoint blockade.

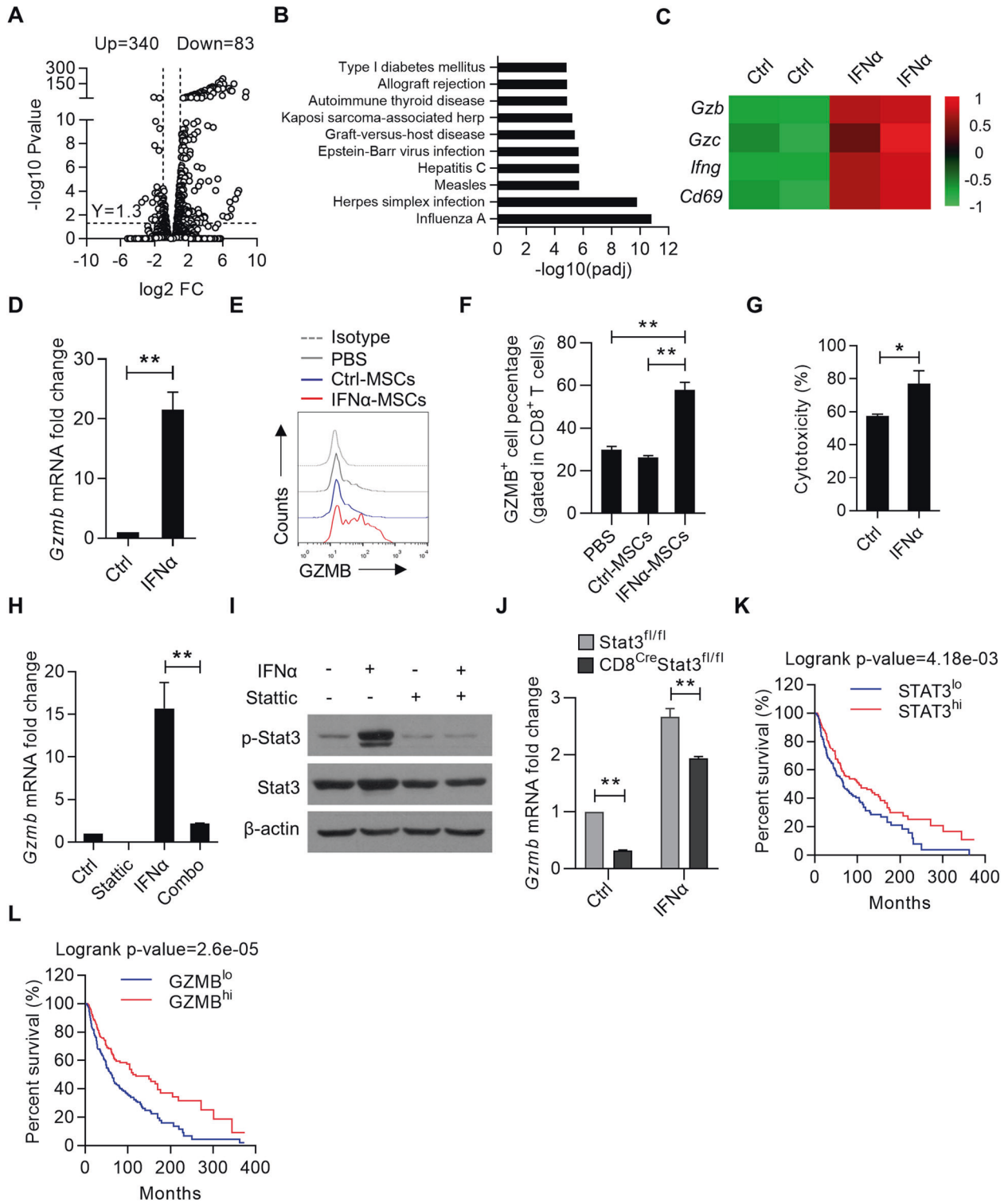
MATERIALS AND METHODS

Study design

The objective of this study was to investigate the therapeutic effect of IFN α -MSCs on tumor progression. To achieve this, we first used TCGA database to analyze the relationship between type I IFNs and their related signals and clinical outcome of patients with melanoma. Second, we constructed IFN α secreting MSCs and tested their anti-tumor effect in explanted and spontaneous tumors. By employment of specific gene knockout mice and antibody to delete certain type of immune cells, we confirmed that CD8⁺ T cells are indispensable for the therapeutic effects of IFN α -MSCs. We further verified the molecular mechanisms of IFN α in treatment of tumors. Last, we explored the synergistic effect of IFN α -MSCs and PD-L1 blockade on the suppression of tumor.

Cells

MSCs were isolated from bone marrow of 6-week-old female C57/BL6 mouse tibia and femur according to the protocol previously described by our laboratory [57]. Ctrl-MSCs and IFN α -MSCs were constructed by lentivirus transfection as previously described [27]. MC38 cells were purchased from Kerafast (Boston, MA). B16F10 cells and MC38 cells were cultured in Dulbecco's modified Eagle's medium supplemented with 10% fetal bovine serum, 2 mM glutamine, 100 U/ml penicillin, and 100 μ g/ml streptomycin. All cell lines were tested negative for Mycoplasma contamination and authenticated with short tandem repeat assays. Splenic or intra-tumoral CD8⁺ T cells were isolated using magnetic cell sorting kit (Miltenyi Biotec, Bergisch Gladbach, Germany). CD8⁺ T cells were cultured in RPMI-1640 medium supplemented with 10% fetal bovine serum, 2 mM glutamine, 100 U/ml penicillin, 100 μ g/ml streptomycin, 1 mM sodium pyruvate, and 55 μ M 2-mercaptoethanol (Gibco, Grand Island, NY).



Mice

C57BL/6 mice were purchased from Shanghai Laboratory Animal Center of the Chinese Academy of Science (Shanghai, China). $\beta 2m^{-/-}$, $Ciita^{-/-}$, $Stat3^{fl/fl}$, and $CD8-Cre$ mice were purchased from Jackson Laboratory. $Rag2^{-/-}$ mice were purchased from Biomedel (Shanghai, China). MMTV-PyMT mice were kindly provided by Dr. Xiaoren Zhang of Shanghai Institute of Nutrition and Health of the Chinese Academy of Sciences. $CD8^{Cre}Stat3^{fl/fl}$ mice were obtained by crossing $Stat3^{fl/fl}$ mice with $CD8-Cre$ mice. All mice were maintained under specific pathogen-free condition and were performed in compliance with NIH Guide for the Care and Use of Laboratory Animals (National Academies Press, 2011) and the ARRIVE

guidelines. Furthermore, all experiments were approved by the Institutional Animal Care and Use Committee of the Institute of Nutrition and Health, Shanghai Institutes for Biological Sciences of Chinese Academy of Sciences. A total of 8-week-old mouse was randomly divided into different groups (6–8 mice/group). The animals successfully inoculated with tumor were included in this study. The animals were excluded if the mice rejected tumors or if the animal died prematurely. Considering sex as a biological variable in research, animals were matched for gender in each experiment. For each animal study, due to powerful anti-tumor activity of IFNα-MSCs, the experimenter could not be blinded to whether the animal was injected with Ctrl-MSCs or IFNα-MSCs. 724 mice were used in this study; C57BL/6

Fig. 6 IFN α -MSCs potentiate CD8⁺ T cell cytotoxicity via the Stat3 signaling. **A** Volcano plot highlighting differentially expressed genes in IFN α treated CD8⁺ T cells compared with controls. CD8⁺ T cells were stimulated with PBS or IFN α (2 000 U/ml) for 48 h and subjected to RNA-seq analysis. **B** Gene ontology analysis of enriched transcripts in IFN α treated CD8⁺ T cells compared with controls. **C** Heatmap of the genes related to the activation and effector of CD8⁺ T cells. **D** The mRNA expression of *Gzmb* in CD8⁺ T cells treated with IFN α (2 000 U/ml) for 48 h. **E, F** Flow cytometric analysis of GZMB expression in tumor infiltrated CD8⁺ T cells. CD8⁺ T cells were isolated from tumor and stimulated by PMA and ionomycin in the presence of brefeldin A (BFA) for 4 h. Flow cytometry was used to analyze the expression of GZMB. **G** The cytotoxicity of intra-tumoral CD8⁺ T cells pretreated with IFN α . CD8⁺ T cells were isolated from B16F0 tumor and stimulated by anti-CD3 and anti-CD28 in the presence or absence of IFN α (2 000 U/ml) for 48 h. Then, CD8⁺ T cells were co-cultured with B16F0 cells at a ratio of 50:1 for 24 h. The cytotoxicity of CD8⁺ T cells was measured by lactate dehydrogenase (LDH) assay. **H** The regulation of STAT3 in IFN α induced *Gzmb* expression. CD8⁺ T cells were treated with IFN α (2 000 U/ml), Stattic (1 μ M), an inhibitor of STAT3, or both for 12 h and determined the *Gzmb* expression by qPCR. **I** The effect of Stattic on STAT3 expression in CD8⁺ T cells. CD8⁺ T cells were treated with IFN α (2000 U/ml), Stattic (1 μ M), an inhibitor of STAT3, or both for 0.5 h and examined the expression of Stat3 and phosphorylated Stat3 by immunoblotting. **J** The role of Stat3 in regulating GZMB expression in CD8⁺ T cells upon IFN α stimulation. CD8⁺ T cells were isolated from Stat3^{fl/fl} and CD8^{Cre}Stat3^{fl/fl} mice and treated with PBS or IFN α (2000 U/ml) for 24 h. Cells were detected for *Gzmb* expression by qPCR. **K** The overall survival analysis in STAT3^{lo} and STAT3^{hi} melanoma patients in TCGA database. **L** The overall survival analysis in GZMB^{lo} and GZMB^{hi} melanoma patients. According to STAT3 or GZMB expression, patients were stratified into two cohorts (cutoff at 25%). Data are shown as means \pm SEM. * p < 0.05 and ** p < 0.01.

mice (n = 600), MMTV-PyMT mice (n = 50), Rag2^{-/-} mice (n = 10), Ciita^{-/-} mice (n = 12), β 2m^{-/-} mice (n = 12), Stat3^{fl/fl} mice (n = 20), and CD8^{Cre}Stat3^{fl/fl} mice (n = 20).

Reagents

Specific antibodies used for flow cytometry: CD3 (11-0031-85), CD45 (11-0451-85), CD4 (45-0042-82), CD8 (17-0081-83), CD11b (17-0112-83), Ly6C (17-5932-82), CD49b (12-5971-82), NK1.1 (17-5941-82), CD69 (17-0691-82), CD25 (17-0251-83), CXCR3 (17-1831-82), CXCR4 (12-9991-82), CD44 (12-0441-83), CD62L (17-0621-83), F4/80 (12-4801-82), CD11c(35-0114-82) were obtained from eBioscience Inc (La Jolla, CA). Antibodies to Ly6G (127616), Ki67 (652410), GZMB (515406), and CCR5 (107008) were purchased from BioLegend Inc (La Jolla, CA). Antibodies to Stat1 (9172 S), p-Stat1 (9171 L), p-Stat3 (9145 S), Stat3 (4904 S) and β -actin (4970 S) were purchased from Cell Signaling Technology (Danvers, MA). Small molecule inhibitors, BAY11-7082, PDTC, and AMG487 were purchased from MedChemExpress (Shanghai, China). Fludarabine, Stattic and FTY720 were obtained from TargetMol (Shanghai, China). Recombinant mouse IFN α were obtained from PBL Assay Science (New Brunswick, NJ). Recombinant mouse CXCL10 were obtained from Thermo Fisher Scientific (Waltham, MA). Mouse Cxcl10 shRNA lentiviral particles (shCxcl10: 5'- TTGATGGTCTTAGA TTCCGGA-3') and overexpressing particles (pSLenti-EGFP-P2APuro-CMV-MCS-3Flag and pSLenti-EGFP-P2APuro-CMV-Cxcl10-3Flag) were purchased from OBiO Technology (Shanghai, China).

Tumor models

B16F0 and MC38 tumor models: B16F0 cells or MC38 cells (1×10^6) were intramuscularly inoculated into outside thigh. Ctrl-MSCs or IFN α -MSCs (1×10^6) were locally injected into peritumoral tissue every 3 days. Mice were inspected daily and euthanized when tumor burden started to significantly affect their mobility. B16F10 mouse melanoma model: B16F10 cells (5×10^5) were intravenously injected into C57BL/6 mice. On day 7, they also received intravenous injection of IFN α -MSCs (5×10^5). Spontaneous mammary cancer model: MMTV-PyMT mice at 4 weeks old were treated with PBS, Ctrl-MSCs (3×10^5) or IFN α -MSCs (3×10^5) twice a week. The survival times of tumor bearing mice were recorded and plotted. Mouse melanoma with α -PD-L1 treatment: B16F0 cells (1×10^6) were intramuscularly inoculated into the outside thigh. On day 5, these mice also received PD-L1 antibody (100 μ g, clone 10F.9G2) and IFN α -MSCs (1×10^6). Tumor volumes (volume = $0.5 \times$ length \times width²) were measured every 2 or 3 days.

Isolation and activation of splenic CD8⁺ T cells

Naive CD8⁺ T cells were isolated from the mouse spleen using immunomagnetic separation beads (Miltenyi Biotec, Bergisch Gladbach, Germany). These CD8⁺ T cells were then seeded into 96-well plates (3×10^5 /well) pre-coated with 2.5 μ g/mL anti-CD3 (16-0032-86, eBioscience) with the addition of soluble 1 μ g/mL anti-CD28 (16-0281-86, eBioscience). The CD8⁺ T cells were activated for 2 or 3 days and used for the respective experiments.

CFSE staining

Naive CD8⁺ T cells were isolated from mouse spleen and were stained with 5 μ M CFSE (Invitrogen, Carlsbad, CA) for 10 min. CFSE-labeled CD8⁺ T cells

were stimulated with anti-CD3 (2.5 μ g/mL) and anti-CD28 (1 μ g/mL) in the presence or absence of IFN α for 72 h. Flow cytometry was used to analyze CFSE intensity reduction as an indicator of cell proliferation.

Stimulation of intra-tumoral CD8⁺ T cells in vitro

B16F0 tumor was homogenized by pressing through 70 μ m cell strainers. After washing and centrifugation, cells were resuspended in 35% Percoll solution and layered on 70% Percoll followed by centrifugation at 2000 rpm for 20 min at room temperature. Lymphocytes were collected from the interface and washed with RPMI-1640 medium. Then, the CD8 MicroBeads kit was used to isolate CD8⁺ T cells according to the manufacturer's instruction. Isolated CD8⁺ T cells were seeded in 96-well plates in the presence of α -CD3/CD28 antibodies or PMA (50 ng/ml) plus ionomycin (1 μ g/ml) and incubated with Brefeldin A (BFA) for 4 h before stained for surface markers and intracellular cytokines.

Cytokine measurement

The levels of IFN α and CXCL10 in serum or culture medium were determined by kits from eBioscience according to manufacturer's indications.

Western blotting analysis

Total protein was extracted from cells with RIPA lysis buffer (Beyotime, Shanghai, China). The protein concentration of each sample was determined by BCA Protein Assay (Thermo Scientific). Twenty μ g proteins were loaded and separated on SDS-PAGE. After transferred onto PVDF membrane and blocked with 5% defatted milk powder, specific primary antibodies against p-Stat1, Stat1, p-Stat3, Stat3, and β -actin were used for specific protein detection and HRP-conjugated secondary antibodies were used to reveal specific bindings. The staining was detected with the ECL system (Millipore).

Real-time PCR

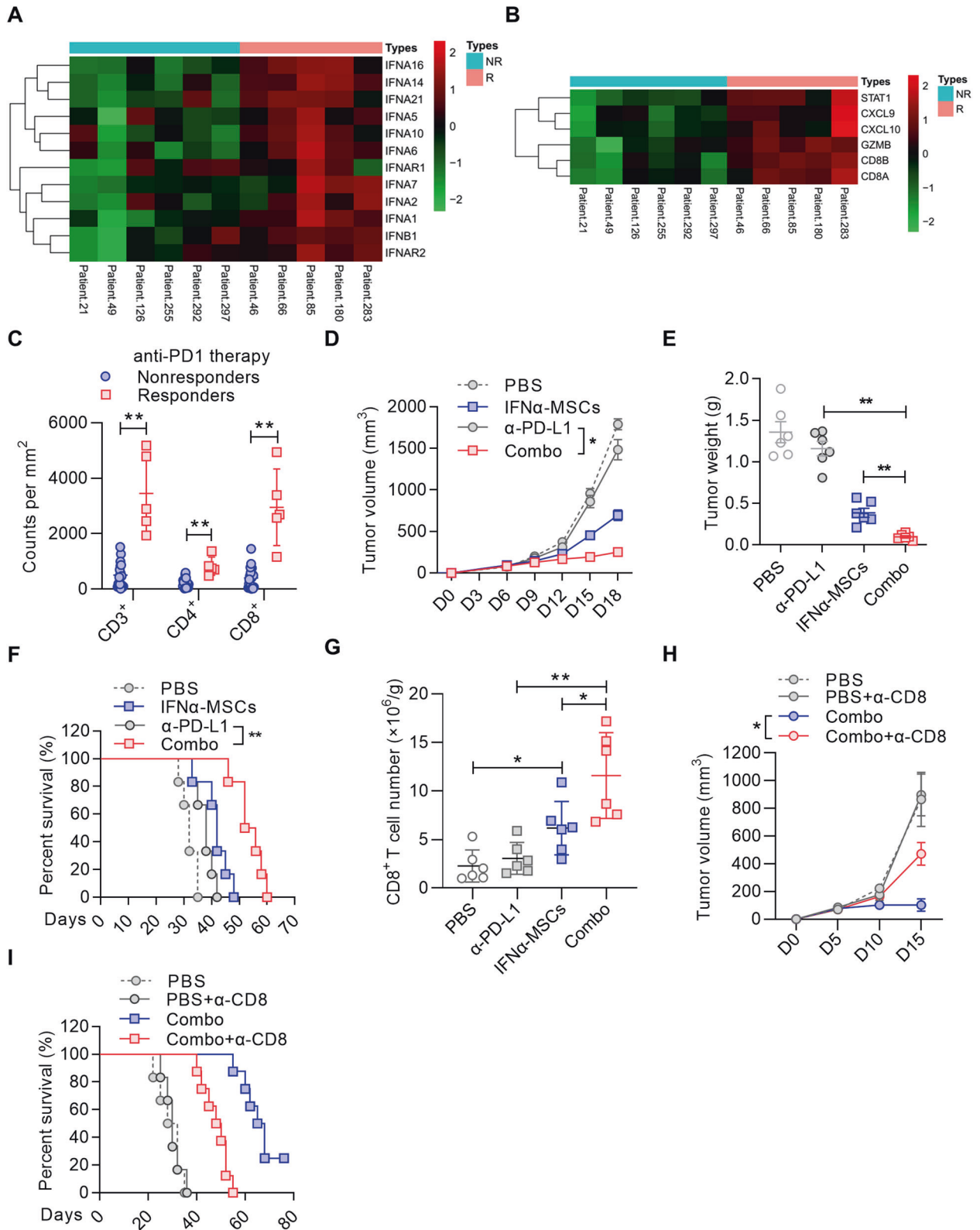
Total RNA was extracted from cells and animal tissues using the Trizol kit (Invitrogen) or RNA easy mini kit (QIAGEN, Hilden, Germany) according to the manufacturer's protocols. qPCR RT master mix kit (Takara, Kyoto, Japan) was used to synthesize cDNA. The qPCR analysis was performed using a FastStart Universal SYBR Green Master (Roche). Sequences of primers used are listed in Supplementary Table 1.

Hematoxylin & eosin and immunofluorescence staining

Tissues from tumor bearing and tumor-free mice were collected and fixed in 4% paraformaldehyde overnight. The samples were sequentially dehydrated with ethanol. After treatment with xylene for 20 min twice, samples were embedded in paraffin. Then, the samples were sectioned at 5 μ m thickness and stained with hematoxylin and eosin. For CD3 staining, the sections were incubated with rabbit anti-CD3 after deparaffinization, followed by incubation with Alexa Fluor 488 conjugated goat anti-rabbit IgG in dark. After DAPI staining, images were taken using a Zeiss Observer Z1 (Carl Zeiss).

Cell cycle and apoptosis analysis

Annexin V/propidium iodide staining (eBioscience) was performed to assess apoptotic and necrotic cells. Briefly, B16F0 cells were treated with



IFN α , Ctrl-MSC CM, or IFN α -MSC CM for 2 days. Annexin V/propidium iodide staining were carried out according to the manufacturer's instructions. Cells were collected and washed with PBS, then analyzed using a BD FACS Caliber flow cytometer (BD Biosciences). The data were analyzed by using FlowJo software.

RNA sequencing and analysis

Naïve splenic CD8⁺ T cells were isolated by immunomagnetic separation beads (Miltenyi Biotec, Bergisch Gladbach, Germany), and stimulated with anti-CD3 and anti-CD28 in the presence or absence of IFN α (2000 U/ml) for 48 h. Total RNA was isolated using Trizol reagent (Ambion). NEBNext[®]

Fig. 7 **IFN α -MSCs synergize with PD-L1 blockade.** **A** Comparison of *IFNA* and *IFNARs* expression in tumors from PD-1 blockade responders and non-responders. **B** Comparison of *STAT1*, *CXCL9*, *CXCL10*, *GZMB*, *CD8B*, and *CD8A* expression in tumors of PD-1 blockade responders and non-responders. **C** The density of CD3⁺, CD4⁺, and CD8⁺ T cells in the tumors of PD-1 blockade responders and non-responders. **D** The synergistic anti-tumor effect of IFN α -MSCs and PD-L1 blockade on tumor growth. B16F0 tumor bearing mice were administered with IFN α -MSCs (1.0×10^6 per mouse, *i.m.*) or α -PD-L1 (100 μ g per mouse, *i.p.*) or both (Combo) on day 5 after tumor initiation. Tumor volume was measured and calculated every 3 days ($n = 4$). **E** Mass of B16F0 tumors treated with IFN α -MSCs, α -PD-L1, or their combination (Combo) ($n = 6$). **F** The survival curves of B16F0 tumor bearing mice treated with IFN α -MSCs, α -PD-L1, or combo ($n = 6$). **G** Numbers of CD8⁺ T cells in the tumors of mice with treatment of IFN α -MSCs, α -PD-L1, or combo ($n = 6$). **H, I** Impairing the synergistic anti-tumor effects of IFN α -MSCs and PD-L1 blockade by CD8⁺ T cell depletion. Mice were inoculated with B16F0 cells and treated with IFN α -MSCs (1.0×10^6) plus α -PD-L1 (100 μ g per mouse), with or without administration of α -CD8 at 200 μ g per mouse ($n = 6$ or 8). Tumor volume was measured and calculated every 5 days (**H**). The survival of B16F0 tumor bearing mice were monitored (**I**). Data are shown as means \pm SEM. * $p < 0.05$, and ** $p < 0.01$.

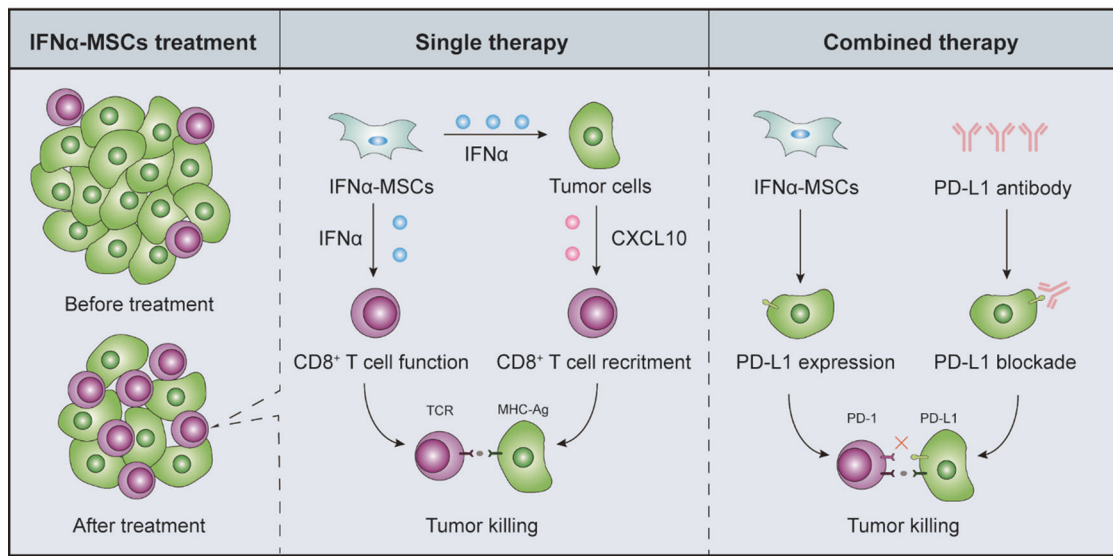


Fig. 8 **Schematic model depicting the mechanisms of anti-tumor effect by IFN α -MSCs.** Administration of IFN α -MSCs stimulates tumor cells to produce CXCL10, which attracts the accumulation of CD8⁺ T cells in tumor sites. IFN α released by IFN α -MSCs also enhances GZMB expression in CD8⁺ T cells and potentiates their anti-tumor activities. More importantly, such remodeling on anti-tumor immune microenvironment by IFN α -MSCs can optimize the therapeutic effect of PD-L1 blockade.

UltraTM RNA Library Prep Kit for Illumina® (NEB, USA) was used for generating sequencing libraries, and samples were sequenced on the Illumina HiSeq platform. Sequencing reads were mapped to the mouse reference genome using Hisat2 v2.0.5. edgeR was used for the normalization and identification of differentially expressed genes. The resulting *P*-values were adjusted using the Benjamini and Hochberg's approach for controlling the false discovery rate. Genes with an adjusted *P*-value < 0.05 and $|\log_2(\text{fold change})| > 1$ were considered as differentially expressed.

Data mining

TCGA-SKCM data was downloaded from the internet (<http://gdac.broadinstitute.org/>). All types of *IFNA* and *IFNARs* were selected for expression analysis. For CD8⁺ T cell infiltration analysis, *IFNAR1*, *IFNAR2*, and *CXCL10* expressions were cut off at 25%. The CIBERSORT analytical tool was used to enumerate CD8⁺ T cell number in melanoma tissues (<https://cibersortx.stanford.edu/>). For survival analysis, *IFNAR1*, *IFNAR2*, *JAK1*, *TYK2*, *STAT1*, *STAT2*, *IRF9*, *MIX1*, *CD8A*, *CXCL10*, *STAT3*, and *GZMB* expressions were cut off at 25% and plotted by using OncoLnc (<http://www.oncolnc.org/>). We used the existing data sets to investigate the link between *IFNA* and *IFNAR* expressions to PD-1 antibody treatment and generated Fig. 7A, B, C [33].

Statistical analysis

Data are presented as means \pm SEM as specified in the figure legends and analyzed with GraphPad Prism 8. The number of mice used per treatment group is indicated as "*n*" in the corresponding figure legends. Student's *t*-test (two tailed) and Log-rank (Mantel-Cox) test were used for statistical analysis. Significant differences are indicated as follows: n.s., no significance, * $p < 0.05$, ** $p < 0.01$, and *** $p < 0.001$.

DATA AVAILABILITY

No statistical methods were used to predetermine sample size. We thus estimated the sample size empirically. No random methods were used in this study. Investigators were not blinded to allocation during experiments. The authors declare that all relevant data of this study are available within the article or from the corresponding author on reasonable request. The RNA-seq data are openly available in Gene Expression Omnibus (GEO), GSE184918.

REFERENCES

- Quail DF, Joyce JA. Microenvironmental regulation of tumor progression and metastasis. *Nat Med*. 2013;19:1423–37.
- Fridman WH, Pages F, Sautes-Fridman C, Galon J. The immune contexture in human tumours: impact on clinical outcome. *Nat Rev Cancer*. 2012;12:298–306.
- Shi Y, Du L, Lin L, Wang Y. Tumour-associated mesenchymal stem/stromal cells: emerging therapeutic targets. *Nat Rev Drug Disco*. 2017;16:35–52.
- Sahai E, Astsaturov I, Cukierman E, DeNardo DG, Egeblad M, Evans RM, et al. A framework for advancing our understanding of cancer-associated fibroblasts. *Nat Rev Cancer*. 2020;20:174–86.
- Hegde PS, Chen DS. Top 10 Challenges in Cancer Immunotherapy. *Immunity*. 2020;52:17–35.
- Tumeh PC, Harview CL, Yearley JH, Shintaku IP, Taylor EJ, Robert L, et al. PD-1 blockade induces responses by inhibiting adaptive immune resistance. *Nature*. 2014;515:568–71.
- Ji RR, Chasalow SD, Wang L, Hamid O, Schmidt H, Cogswell J, et al. An immune-activating tumor microenvironment favors clinical response to ipilimumab. *Cancer Immunol Immunother*. 2012;61:1019–31.
- Ayers M, Lunceford J, Nebozhyn M, Murphy E, Loboda A, Kaufman DR, et al. IFN-gamma-related mRNA profile predicts clinical response to PD-1 blockade. *J Clin Invest*. 2017;127:2930–40.

9. Binnewies M, Roberts EW, Kersten K, Chan V, Fearon DF, Merad M, et al. Understanding the tumor immune microenvironment (TIME) for effective therapy. *Nat Med.* 2018;24:541–50.
10. Chen DS, Mellman I. Elements of cancer immunity and the cancer-immune set point. *Nature.* 2017;541:321–30.
11. Mariathasan S, Turley SJ, Nickles D, Castiglioni A, Yuen K, Wang Y, et al. TGFbeta attenuates tumour response to PD-L1 blockade by contributing to exclusion of T cells. *Nature.* 2018;554:544–8.
12. Kather JN, Suarez-Carmona M, Charoentong P, Weis CA, Hirsch D, Bankhead P et al. Topography of cancer-associated immune cells in human solid tumors. *Elife.* 2018;7:e36967.
13. Herbst RS, Soria JC, Kowanzet M, Fine GD, Hamid O, Gordon MS, et al. Predictive correlates of response to the anti-PD-L1 antibody MPDL3280A in cancer patients. *Nature.* 2014;515:563–7.
14. Liang Y, Tang H, Guo J, Qiu X, Yang Z, Ren Z, et al. Targeting IFNalpha to tumor by anti-PD-L1 creates feedforward antitumor responses to overcome checkpoint blockade resistance. *Nat Commun.* 2018;9:4586.
15. Fuertes MB, Kacha AK, Kline J, Woo SR, Kranz DM, Murphy KM, et al. Host type I IFN signals are required for antitumor CD8+ T cell responses through CD8alpha+ dendritic cells. *J Exp Med.* 2011;208:2005–16.
16. Diamond MS, Kinder M, Matsushita H, Mashayekhi M, Dunn GP, Archambault JM, et al. Type I interferon is selectively required by dendritic cells for immune rejection of tumors. *J Exp Med.* 2011;208:1989–2003.
17. Sistigu A, Yamazaki T, Vacchelli E, Chaba K, Enot DP, Adam J, et al. Cancer cell-autonomous contribution of type I interferon signaling to the efficacy of chemotherapy. *Nat Med.* 2014;20:1301–9.
18. Yang X, Zhang X, Fu ML, Weichselbaum RR, Gajewski TF, Guo Y, et al. Targeting the tumor microenvironment with interferon-beta bridges innate and adaptive immune responses. *Cancer Cell.* 2014;25:37–48.
19. Burnette BC, Liang H, Lee Y, Chlewicki L, Khodarev NN, Weichselbaum RR, et al. The efficacy of radiotherapy relies upon induction of type I interferon-dependent innate and adaptive immunity. *Cancer Res.* 2011;71:2488–96.
20. Deng L, Liang H, Xu M, Yang X, Burnette B, Arina A, et al. STING-dependent cytosolic DNA sensing promotes radiation-induced type I interferon-dependent antitumor immunity in immunogenic tumors. *Immunity.* 2014;41:843–52.
21. Robb RJ, Kreijveld E, Kuns RD, Wilson YA, Olver SD, Don AL, et al. Type I IFNs control GVHD and GVL responses after transplantation. *Blood.* 2011;118:3399–409.
22. Pardoll DM. The blockade of immune checkpoints in cancer immunotherapy. *Nat Rev Cancer.* 2012;12:252–64.
23. Pestka S. The interferons: 50 years after their discovery, there is much more to learn. *J Biol Chem.* 2007;282:20047–51.
24. Bracarda S, Eggermont AM, Samuelsson J. Redefining the role of interferon in the treatment of malignant diseases. *Eur J Cancer.* 2010;46:284–97.
25. Talantov D, Mazumder A, Yu JX, Briggs T, Jiang Y, Backus J, et al. Novel genes associated with malignant melanoma but not benign melanocytic lesions. *Clin Cancer Res: Off J Am Assoc Cancer Res.* 2005;11:7234–42.
26. Newman AM, Liu CL, Green MR, Gentles AJ, Feng W, Xu Y, et al. Robust enumeration of cell subsets from tissue expression profiles. *Nat Methods.* 2015;12:453–7.
27. Xu C, Lin L, Cao G, Chen Q, Shou P, Huang Y, et al. Interferon-alpha-secreting mesenchymal stem cells exert potent antitumor effect in vivo. *Oncogene.* 2014;33:5047–52.
28. Shou P, Chen Q, Jiang J, Xu C, Zhang J, Zheng C, et al. Type I interferons exert anti-tumor effect via reversing immunosuppression mediated by mesenchymal stromal cells. *Oncogene.* 2016;35:5953–62.
29. Chang CH, Guerder S, Hong SC, van Ewijk W, Flavell RA. Mice lacking the MHC class II transactivator (CIITA) show tissue-specific impairment of MHC class II expression. *Immunity.* 1996;4:167–78.
30. Zijlstra M, Bix M, Simister NE, Loring JM, Raulet DH, Jaenisch R. Beta 2-microglobulin deficient mice lack CD4-8+ cytolytic T cells. *Nature.* 1990;344:742–6.
31. Yeruva S, Ramadori G, Raddatz D. NF-kappaB-dependent synergistic regulation of CXCL10 gene expression by IL-1beta and IFN-gamma in human intestinal epithelial cell lines. *Int J Colorectal Dis.* 2008;23:305–17.
32. Riaz N, Havel JJ, Makarov V, Desrichard A, Urba WJ, Sims JS, et al. Tumor and microenvironment evolution during immunotherapy with nivolumab. *Cell.* 2017;171:934–949.
33. Chen PL, Roh W, Reuben A, Cooper ZA, Spencer CN, Prieto PA, et al. Analysis of immune signatures in longitudinal tumor samples yields insight into biomarkers of response and mechanisms of resistance to immune checkpoint blockade. *Cancer Disco.* 2016;6:827–37.
34. Bazhin AV, von Ahn K, Fritz J, Werner J, Karakhanova S. Interferon-alpha upregulates the expression of PD-L1 molecules on immune cells through STAT3 and p38 signaling. *Front Immunol.* 2018;9:2129.
35. Zitvogel L, Galluzzi L, Kepp O, Smyth MJ, Kroemer G. Type I interferons in anticancer immunity. *Nat Rev Immunol.* 2015;15:405–14.
36. Valastyan S, Weinberg RA. Tumor metastasis: molecular insights and evolving paradigms. *Cell.* 2011;147:275–92.
37. Steeg PS. Tumor metastasis: mechanistic insights and clinical challenges. *Nat Med.* 2006;12:895–904.
38. Cristescu R, Mogg R, Ayers M, Albright A, Murphy E, Yearley J, et al. Pan-tumor genomic biomarkers for PD-1 checkpoint blockade-based immunotherapy. *Science.* 2018;362:eaar3593.
39. Galon J, Bruni D. Approaches to treat immune hot, altered and cold tumours with combination immunotherapies. *Nat Rev Drug Disco.* 2019;18:197–218.
40. Bald T, Landsberg J, Lopez-Ramos D, Renn M, Glodde N, Jansen P, et al. Immune cell-poor melanomas benefit from PD-1 blockade after targeted type I IFN activation. *Cancer Disco.* 2014;4:674–87.
41. Guo J, Xiao Y, Iyer R, Lu X, Lake M, Lador U, et al. Empowering therapeutic antibodies with IFN-alpha for cancer immunotherapy. *PLoS One.* 2019;14:e0219829.
42. Fend L, Yamazaki T, Remy C, Fahrner C, Gantzer M, Nourtier V, et al. Immune checkpoint blockade, immunogenic chemotherapy or IFN-alpha blockade boost the local and abscopal effects of oncolytic virotherapy. *Cancer Res.* 2017;77:4146–57.
43. Delaunay T, Achard C, Boisgerault N, Grard M, Petithomme T, Chatelain C, et al. Frequent homozygous deletions of type I interferon genes in pleural mesothelioma confer sensitivity to oncolytic measles virus. *J Thorac Oncol.* 2020;15:827–42.
44. Aref S, Castleton AZ, Bailey K, Burt R, Dey A, Leongamornlert D, et al. Type 1 interferon responses underlie tumor-selective replication of oncolytic measles virus. *Mol Ther.* 2020;28:1043–55.
45. Groom JR, Luster AD. CXCR3 in T cell function. *Exp Cell Res.* 2011;317:620–31.
46. Chheda ZS, Sharma RK, Jala VR, Luster AD, Haribabu B. Chemoattractant receptors BLT1 and CXCR3 regulate antitumor immunity by facilitating CD8+ T cell migration into tumors. *J Immunol.* 2016;197:2016–26.
47. Kawada K, Sonoshita M, Sakashita H, Takabayashi A, Yamaoka Y, Manabe T, et al. Pivotal role of CXCR3 in melanoma cell metastasis to lymph nodes. *Cancer Res.* 2004;64:4010–7.
48. Wightman SC, Uppal A, Pitroda SP, Ganai S, Burnette B, Stack M, et al. Oncogenic CXCL10 signalling drives metastasis development and poor clinical outcome. *Br J Cancer.* 2015;113:327–35.
49. Doron H, Amer M, Ershaid N, Blazquez R, Shani O, Lahav TG, et al. Inflammatory activation of astrocytes facilitates melanoma brain tropism via the CXCL10-CXCR3 signaling axis. *Cell Rep.* 2019;28:1785–98.
50. Cauwels A, Van Lint S, Paul F, Garcin G, De Koker S, Van, et al. Delivering type I interferon to dendritic cells empowers tumor eradication and immune combination treatments. *Cancer Res.* 2018;78:463–74.
51. Tsuchiya N, Zhang R, Iwama T, Ueda N, Liu T, Tatsumi M, et al. Type I interferon delivery by iPSC-derived myeloid cells elicits antitumor immunity via XCR1(+) dendritic cells. *Cell Rep.* 2019;29:162–75.
52. Paolini R, Bernardini G, Molfetta R, Santoni A. NK cells and interferons. *Cytokine Growth Factor Rev.* 2015;26:113–20.
53. Muller E, Speth M, Christopoulos PF, Lunde A, Avdagic A, Oynebraten I, et al. Both type I and type II interferons can activate antitumor M1 macrophages when combined with TLR stimulation. *Front Immunol.* 2018;9:2520.
54. Tecchio C, Huber V, Scapini P, Calzetti F, Margotto D, Todeschini G, et al. IFNalpha-stimulated neutrophils and monocytes release a soluble form of TNF-related apoptosis-inducing ligand (TRAIL/Apo-2 ligand) displaying apoptotic activity on leukemic cells. *Blood.* 2004;103:3837–44.
55. Mohty M, Vialle-Castellano A, Nunes JA, Isnardon D, Olive D, Gaugler B. IFN-alpha skews monocyte differentiation into Toll-like receptor 7-expressing dendritic cells with potent functional activities. *J Immunol.* 2003;171:3385–93.
56. Montoya M, Schiavoni G, Mattei F, Gresser I, Belardelli F, Borrow P, et al. Type I interferons produced by dendritic cells promote their phenotypic and functional activation. *Blood.* 2002;99:3263–71.
57. Ren G, Zhang L, Zhao X, Xu G, Zhang Y, Roberts AI, et al. Mesenchymal stem cell-mediated immunosuppression occurs via concerted action of chemokines and nitric oxide. *Cell Stem Cell.* 2008;2:141–50.

ACKNOWLEDGEMENTS

The study was supported by grants from the National Key R&D Program of China (2018YFA0107500), the Scientific Innovation Project of the Chinese Academy of Sciences (XDA16020403), the National Natural Science Foundation of China (32070872, 31961133024, 31771641, 81571612, 31771581 and 81861138015), a start-up fund from Soochow University, and the Department of Science and Technology of Jiangsu Province research fund (BE2016671).

AUTHOR CONTRIBUTIONS

TZ designed and performed the experiments. YW, LL, QL, CX, YX., and MH helped conduct experiments and revised manuscript. YW and YS led the project and revised the manuscript.

COMPETING INTERESTS

The authors declare no competing interests.

ADDITIONAL INFORMATION

Supplementary information The online version contains supplementary material available at <https://doi.org/10.1038/s41388-022-02201-4>.

Correspondence and requests for materials should be addressed to Yufang Shi or Ying Wang.

Reprints and permission information is available at <http://www.nature.com/reprints>

Publisher's note Springer Nature remains neutral with regard to jurisdictional claims in published maps and institutional affiliations.



Open Access This article is licensed under a Creative Commons Attribution 4.0 International License, which permits use, sharing, adaptation, distribution and reproduction in any medium or format, as long as you give appropriate credit to the original author(s) and the source, provide a link to the Creative Commons license, and indicate if changes were made. The images or other third party material in this article are included in the article's Creative Commons license, unless indicated otherwise in a credit line to the material. If material is not included in the article's Creative Commons license and your intended use is not permitted by statutory regulation or exceeds the permitted use, you will need to obtain permission directly from the copyright holder. To view a copy of this license, visit <http://creativecommons.org/licenses/by/4.0/>.

© The Author(s) 2022